

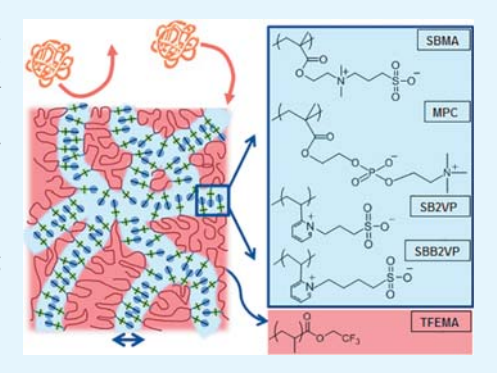
Self-Assembling Zwitterionic Copolymers as Membrane Selective Layers with Excellent Fouling Resistance: Effect of Zwitterion Chemistry

Prity Bengani-Lutz, † Elisha Converse, † Peggy Cebe, † and Ayse Asatekin*, † [b]

[†]Tufts University, Department of Chemical and Biological Engineering, 4 Colby Street, Medford, Massachusetts 02155, United States [‡]Tufts University, Department of Physics and Astronomy, 574 Boston Avenue, Medford, Massachusetts 02155, United States

Supporting Information

ABSTRACT: Membranes with high flux, ~1 nm pore size, and unprecedented protein fouling resistance were prepared by forming selective layers of selfassembling zwitterionic amphiphilic random copolymers on porous supports by a simple coating method. Random copolymers were prepared from the hydrophobic monomer 2,2,2-trifluoroethyl methacrylate (TFEMA) and four zwitterionic monomers (sulfobetaine methacrylate, sulfobetaine 2-vinylpyridine, sulfobutylbetaine 2-vinylpyridine, and 2-methacryloyloxyethyl phosphorylcholine) by free radical polymerization. All copolymers microphase separated to form bicontinuous ~1.2 nm nanodomains with the zwitterionic domains acting as nanochannels for the permeation of water and solutes. The resultant membranes all had a ~1 nm size cutoff independent of zwitterion chemistry. There were, however, significant differences in the hydrophilicity, water uptake, water flux, and fouling resistance among membranes prepared with different



zwitterionic monomers. Membranes prepared from the copolymer with 2-methacryloyloxyethyl phosphorylcholine were the most hydrophilic and had the highest water permeance, higher than that of commercial membranes of similar pore size. Furthermore, these membranes showed unprecedented fouling resistance, exhibiting no measurable flux decline throughout a 24 h protein fouling experiment. The structure-property relationships gleaned from this survey of different zwitterion structures serves as a guideline to develop new zwitterionic materials for various applications such as membranes, drug delivery, and sensors.

KEYWORDS: ultrafiltration, nanofiltration, fouling, zwitterion, self-assembly, membrane, sulfobetaine, phosphorylcholine

1. INTRODUCTION

Membranes are an energy efficient, environmentally friendly, modular separation technology that offers a small footprint and higher effluent quality compared to other conventional separation processes. While these advantages have led to their established use in applications such as water and wastewater treatment, their broader use is limited by limitations in separations achievable by existing products. Membrane separations are typically characterized based on the membrane pore size. Membranes with pores in the \sim 1 nm range are useful for numerous applications, including textile wastewater treatment, pharmaceutical purification, and bioseparations. However, there are very few commercial membranes available in this pore size range, and those that are available show poor selectivity between desired components due to broad pore size distributions. They also often have a charged surface, which leads to rejections being affected by solute size, charge, and chemical interactions between the solute and the membrane. Furthermore, most commercial membranes suffer from low fluxes and high fouling.⁴ Fouling is the loss of membrane permeability caused by adhesion and accumulation of feed components on the membrane surface.⁵ Fouling results in a decline in flux, leading to reduced productivity and increased

energy costs. Thus, new fouling-resistant membrane chemistries are needed.

Whitesides and coworkers screened self-assembling monolayers (SAMs) with 60 different surface chemistries⁶ and found that surfaces that resist protein adsorption successfully share 4 molecular level characteristics: they are hydrophilic, hydrogen acceptors, not hydrogen donors, and are neutral in charge. These criteria suggest several promising antifouling chemistries, including poly(ethylene glycol) (PEG),7 mannitol groups,8 chimeric peptoids,9 and zwitterions.7,10,11 Among these, zwitterions, neutral species with equal number of cationic and anionic moieties located on the same molecule, are a promising option. They are chemically stable, and their performance is comparable to, and in some cases better than, PEG-based systems for resisting protein adsorption^{7,10-14} and bacterial adhesion. 10,11 While the mechanism is not fully understood, the fouling resistance is attributed to the preservation of water structure and a high degree of hydration around zwitterions via strong electrostatic interactions in addition to hydrogen

Received: April 6, 2017 Accepted: May 25, 2017

Published: May 25, 2017

ACS Applied Materials & Interfaces

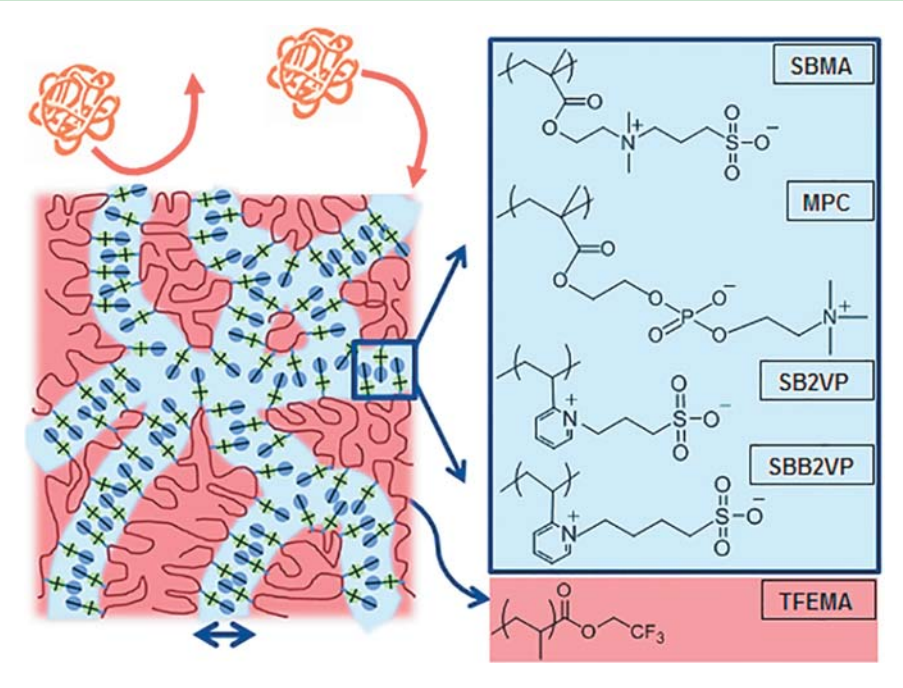


Figure 1. Left: Schematic showing the self-assembly of zwitterionic amphiphilic random copolymers to form a network of water-permeable effective "nanochannels" and the interaction of membranes whose selective layers they form with foulants (orange). Right: chemical structures of the repeat units forming the copolymers used in this study. Zwitterionic repeat units: SBMA, MPC, SB2VP, and SBB2VP; hydrophobic repeat unit: TFEMA.

bonding. 15,16 This leads to a large energy barrier to foulant adsorption on the surface. 17-23

Another important feature of zwitterionic materials is their strong tendency to self-assemble, driven by strong dipoledipole interactions. Due to the presence of strong electrostatic interactions, these dipoles are expected to arrange in an antiparallel fashion to form tubular or disk-like structures rather than spheres. 19,23 Random copolymers of zwitterions are shown to form $\sim 1-5$ nm sized clusters. ²⁴⁻²⁷ On the basis of this premise, we recently reported a new class of membranes using self-assembling random amphiphilic copolymers as selective layers.²⁸ It was shown that random copolymers of a zwitterionic monomer, sulfobetaine methacrylate (SBMA), and a hydrophobic monomer (2,2,2-trifluoroethyl methacrylate (TFEMA), methyl methacrylate (MMA), or acrylonitrile) self-assemble to form effective domains or nanochannels that are ~1 nm in size (Figure 1). Membranes whose selective layers are composed of these polymers, prepared by coating a porous support with a thin film, have effective pore sizes that match this domain size, corresponding to a molecular weight cutoff (MWCO) of about 1000 Da. These membranes are also very fouling-resistant against proteins and oil emulsions. However, only one zwitterionic monomer was tested due to ease of commercial

Zwitterions comprise a large library of molecules with different anionic and cationic species, 29 but relatively little is known about the differences between different zwitterionic materials. Studies based on zwitterionic surfactants and simulations have shown that zwitterionic molecules with different functional groups and varying distance between the charged groups can have different hydration structures, hydration dynamics, and degrees of interactions with water.30-38 It was suggested that highly protein resistant surfaces should have few to moderate self-associations and fewer interactions with proteins in addition to a strong hydration layer to make protein adsorption unfavorable.

Similar studies on how zwitterion chemistry affects copolymer self-assembly are lacking overall.

To date, most studies on zwitterion chemistry and fouling resistance compare the same two monomers: carboxybetaine methacrylate (CBMA) and sulfobetaine methacrylate (SBMA), each containing a quaternary ammonium as the cation and either a carboxylic group or a sulfonate group, respectively, as the anion. $^{14,39-43}$ They found that membranes grafted with poly(CBMA) or poly(SBMA) both showed good resistance to platelet adhesion. 44 Phosphorylcholines, another important class of zwitterions with a phosphate anionic group, also have strong hydration layers, 15,16,45 but simulations or studies comparing them to other zwitterionic materials are lacking. The broad diversity of available zwitterionic groups, functional groups that attach charged groups to the polymer backbone, and the distance between charged groups can potentially alter the performance of membranes prepared from their random copolymers described earlier. Furthermore, these membrane systems may be ideal in better understanding links between zwitterion chemistry, fouling resistance, and self-assembly.

In this work, we report the effect of varying zwitterion chemical structure on the self-assembly of random amphiphilic zwitterionic copolymers and the performance of membranes whose selective layer they form (Figure 1). We performed a systematic study of four zwitterionic chemical structures by varying the zwitterion type (sulfobetaine vs phosphorylcholine), chain length between the charges of the zwitterionic monomer (spacer length), and the groups that link the first charged functional group of the zwitterion to the polymer backbone (linker). We show that, for similar zwitterionic repeat unit content in these copolymers, membranes formed from these copolymers may have very different permeability and fouling resistance behaviors. These differences in membrane performance are attributed to the different chemical structures, hydration, and relative hydrophilicities of the zwitterionic groups in the copolymer. These results are in good agreement with contact angle and copolymer water uptake measurements. The structure-property relationships and design principles developed here can serve as a guideline to develop new zwitterionic materials for various applications such as membrane filtration, drug delivery, and other applications relying on protein-resistant interfaces.

2. EXPERIMENTAL SECTION

2.1. Materials. Azobis(isobutyronitrile) (AIBN), 4-methoxy phenol (MEHQ), sulfobetaine methacrylate (SBMA), 2-methacryloyloxyethyl phosphorylcholine (MPC), 1,3-propane sultone, 1,4-butane sultone, bovine serum albumin (BSA, 66.5 kDa), phosphate buffered saline (PBS) packets, and all dyes were purchased from Sigma-Aldrich. 2,2,2-Trifluoroethyl methacrylate (TFEMA) was obtained from Scientific Polymer Products Inc. Trifluoroethanol (TFE), dimethyl sulfoxide (DMSO), tetrahydrofuran (THF), acetonitrile, isopropanol (IPA), ethanol, benzene, hexane, copper(II) chloride (CuCl₂), lithium chloride (LiCl), and basic activated alumina were purchased from VWR. Deuterated solvents such as deuterium oxide (D2O) and deuterated dimethyl sulfoxide (DMSO-d₆) were obtained from Cambridge Isotope Laboratory. All chemicals and solvents were reagent grade and used as received except TFEMA, which was purified by passing through a column of basic activated alumina. PVDF 400R ultrafiltration membranes purchased from Nanostone Water (Eden Prairie, MN) were used as the base membrane. Poly(ether sulfone) (PES) 1000 Da molecular weight cutoff (MWCO) membranes (Sartorius) were purchased from Fisher Scientific Inc. (Pittsburgh, PA) and used as a control. Deionized water supplied by Biolab 3300 RO, a building-wide reverse osmosis/deionized water (RO/DI) purification unit by Mar Cor Purification was used for all experiments.

2.2. Synthesis of Zwitterionic Monomers and Amphiphilic Zwitterionic Copolymers. 2.2.1. Synthesis of PTFEMA-r-SBMA (PT:SBMA) Copolymer. PT:SBMA was synthesized by free radical polymerization (FRP) using a previously published procedure with small modifications.²⁸ Lithium chloride (0.1 g) was dissolved in 80 mL of dimethyl sulfoxide by stirring in a round-bottomed flask. Four grams of SBMA was added to the flask and dissolved in the solution by stirring, followed by TFEMA (six grams) and AIBN (0.01 g). The flask was sealed with a rubber septum, purged with nitrogen for 20 min, and placed in an oil bath at 70 °C with stirring. After 20 h, the flask was removed from the oil bath. MEHQ (0.5 g) was added to the flask to terminate the reaction. Copolymer was precipitated in a 50:50 mixture of ethanol and hexane. The product was vacuum filtered, and remaining solvent and monomers were extracted by stirring the polymer in a methanol bath twice for at least 8 h. The final product was dried in the vacuum oven overnight at 50 °C. The copolymer composition was determined by ¹H NMR spectroscopy.

2.2.2. Synthesis of PTFEMA-r-MPC (PT:MPC) Copolymer. PT:MPC was also synthesized by FRP using a similar procedure. Three grams of MPC was dissolved in 65 mL of ethanol by stirring in a roundbottomed flask. TFEMA (7 g) and AIBN (0.01 g) were added. The flask was sealed with a rubber septum, purged with nitrogen for 20 min, and placed in an oil bath at 70 °C with stirring. The flask and oil bath setup was covered with aluminum foil as the MPC monomer is reported to be somewhat light sensitive. After 20 h, the flask was removed from the oil bath. 4-MEHQ (0.5 g) was added to the flask to terminate the reaction. Copolymer was precipitated in tetrahydrofuran. The product was vacuum filtered, and remaining solvent and monomers were extracted by stirring the polymer in a tetrahydrofuran bath twice for at least 8 h. The final product was dried in the vacuum oven overnight at 50 °C. The copolymer composition was determined by ¹H NMR spectroscopy.

2.2.3. Synthesis of PTFEMA-r-SB2VP (PT:SB2VP) Copolymer. SB2VP monomer was synthesized using a slightly modified version of the procedure published in the literature. 46 It is a quaternization reaction of 2-vinylpyridine with 1,3-propane sultone (Scheme 1). 2-Vinylpyridine (25 mL, 0.238 mol) and 1,3-propane sultone (25 mL, 0.205 mol) were dissolved in 250 mL acetonitrile in a round-bottomed flask. The flask was sealed with a rubber septum, purged with nitrogen

Scheme 1. Reaction Scheme Showing Synthesis of Pyridinium-Based Sulfobetaine Monomers (SB2VP and SBB2VP) by Quaternization Reaction of 2-Vinylpyridine with 1,3-Propane Sultone or 1,4-Butane Sultone

gas for 60 min, and placed in an oil bath at 60 $^{\circ}\text{C}$ with stirring. Within a few hours, a light yellow precipitate was observed in the flask. After 3 days, the flask was removed from the oil bath. The product was vacuum filtered, and remaining solvent and monomers were extracted by stirring the monomer in a diethyl ether bath twice for at least 8 h. The final product was dried overnight in a chemical hood at room temperature. The monomer composition was determined by ¹H NMR spectroscopy.

PT:SB2VP was synthesized by FRP using a procedure similar to that for other copolymers. Five grams of SB2VP was dissolved in 65 mL of trifluoroethanol by stirring in a round-bottomed flask. TFEMA (5 g) and AIBN (0.01 g) were added. The flask was sealed with a rubber septum, purged with nitrogen gas for 20 min, and placed in an oil bath at 70 °C with stirring. After 20 h, the flask was removed from the oil bath. MEHQ (0.5 g) was added to the flask to terminate the reaction. Copolymer was precipitated in ethanol. The product was vacuum filtered, and remaining solvent and monomers were extracted by stirring the polymer in water bath twice for at least 8 h. The final product was dried in the vacuum oven overnight at 50 °C. The copolymer composition was determined by ¹H NMR spectroscopy.

2.2.4. Synthesis of PTFEMA-r-SBB2VP (PT:SBB2VP) Copolymer. SBB2VP monomer was synthesized (Scheme 1) using a significantly modified version of the procedure previously published in the literature.⁴⁷ 2-Vinylpyridine (100 mL, 0.951 mol) and 1,4-butane sultone (120 mL, 0.881 mol) were dissolved in 500 mL of benzene in a round-bottomed flask. 1,4-Butane sultone was added. Dinitrobenzene (100 mg) was added to inhibit polymerization. The neck of the flask was greased and connected to a water-cooled reflux column with the lower inlet tubing connected to cold water line in the fume hood. Water flow was maintained to continuously reflux the solvent without loss of mass. A similar experiment was performed separately using compressed air flow to cool the column instead of water with similar results. The column was sealed with a rubber septum and purged with nitrogen continuously. The flask was placed in an oil bath and refluxed at 80 °C with stirring. After approximately 2 h, a light yellow precipitate was observed in the flask. After 5 days, the water flow was stopped, and the flask was removed from the oil bath. The product was vacuum filtered, and remaining solvent and unreacted monomers were extracted by washing in diethyl ether thrice for at least 8 h. The final product was dried overnight in a chemical hood at room temperature. The monomer composition was determined by ¹H NMR spectrosco-

PT:SBB2VP was synthesized by FRP using a procedure similar to that for other copolymers. Five grams of SBB2VP was dissolved in 60 mL of trifluoroethanol by stirring in a round-bottomed flask. TFEMA (5 g) and AIBN (0.01 g) were added. The flask was sealed with a rubber septum, purged with nitrogen gas for 20 min, and placed in an oil bath at 70 $^{\circ}\text{C}$ with stirring. After 20 h, the flask was removed from the oil bath. MEHQ (0.5 g) was added to the flask to terminate the reaction. Copolymer was precipitated in water. The product was vacuum filtered, and remaining solvent and monomers were extracted by stirring the polymer in an ethanol bath twice for at least 8 h. The final product was dried in the vacuum oven overnight at 50 °C. The copolymer composition was determined by ¹H NMR spectroscopy.

2.2.5. Characterization of Molecular Weight. To characterize the molecular weight of copolymers, dynamic light scattering (DLS, Brookhaven Instruments Nanobrook ZetaPALS) was performed using a 35 mW red diode laser with a nominal wavelength of 659 nm as the

light source. All of the measurements were done on 1 mg/mL copolymer solutions in TFE at a scattering angle of 90° and a temperature of 25 °C controlled by a thermostat. A 0.2 μ m filter was used to remove dust before light scattering experiments. After stabilization of samples for 2 min, 3 measurements were performed for each copolymer. The effective hydrodynamic radius and relative molecular weight based on polyacrylonitrile (PAN) standards in dimethylformamide (DMF) were determined by the instrument software (BIC Particle Solutions v. 2.5).

2.3. Characterization of Self-Assembled Morphology. 2.3.1. Transmission Electron Microscopy (TEM). To characterize the self-assembled nanostructure of these zwitterionic amphiphilic random copolymers, TEM was performed. Images were obtained using a FEI Technai Spirit transmission electron microscope in bright field mode operated at 80 keV. Films of PT:SBMA, PT:MPC, PT:SB2VP, and PT:SBB2VP copolymers were cast by pouring 10% (w/v), 12% (w/v), 15% (w/v), and 15% (w/v) solutions of each copolymer in TFE, respectively, into Teflon dishes and evaporating the solvent overnight. Zwitterionic domains were positively stained with CuCl₂ utilizing the formation of stable complexes between copper and zwitterions. ⁴⁸ Following a procedure previously published, ²⁸ these copolymer films were immersed in 2% copper(II) chloride (CuCl₂) solution for 4 h, dabbed with a filter paper to remove excess, followed by water immersion for 5 min. Once stained, the films were dried and embedded in EMbed 812 epoxy resin for two nights with frequent epoxy replacement. Ultrathin ~50 nm sections were cut using an ultramicrotome and placed on copper grids (200 mesh, Electron Microscopy Sciences). Image acquisition was carried out by Dr. Nicki Watson at W. M. Keck foundation Biological Imaging Facility at the Whitehead Institute. Fast Fourier transform was performed on these images using ImageJ software.

2.3.2. Water Uptake. To measure copolymer water uptake, ~ 40 mg of solvent-cast films of each of the four copolymers, PT:SBMA, PT:MPC, PT:SB2VP, PT:SBB2VP, were weighed in their dry state, and immersed in deionized water. After 24 h, the samples were removed, dabbed with a lint-free wipe to remove any residual water, and weighed again. The difference between the final and initial weight normalized by the initial dry weight was calculated to obtain water uptake (wt %).

2.3.3. Differential Scanning Calorimetry (DSC). To characterize the copolymer phase morphology and thermal properties, we performed temperature modulated DSC (TMDSC). Measurements were obtained using a TA Instruments Q100 series DSC equipped with a refrigerated cooling system. Polymer samples were dried for at least 24 h in a vacuum oven at 50 °C. Five to ten milligrams of each sample was measured in a standard aluminum DSC pan sealed with a standard aluminum lid. A blank pan and lid of comparable weight was used as a reference. The DSC cell was purged with nitrogen at a flow rate of 50 mL min⁻¹. All sample measurements were performed under the same TMDSC conditions: equilibrate at 60 °C, isothermal for 10 min, equilibrate at -80 °C, hold isothermally for 5 min, modulate ± 1 °C every 40 s, hold isothermally for 5 min, and finally ramp 3 °C/min to 250 °C. Analysis of TMDSC data was performed using TA Instruments Universal Analysis 2000 and MATLAB programs (Mathworks). To calculate the theoretical mixed-phase $T_{\rm g}$ of the copolymers $(T_{\rm g}^{\rm cop})$, we used the Fox equation, ⁴⁹ which assumes that in a copolymer blend the free volume is proportional to the weight fraction of each repeat unit:

$$\frac{1}{T_{g^{cop}}} = \frac{w_{A}}{T_{g^{A}}} + \frac{w_{B}}{T_{g^{B}}} \tag{1}$$

where T_{σ}^{A} is the T_{σ} of poly(trifluoroethyl methacrylate), T_{σ}^{B} is the T_{σ} of the homopolymer of the zwitterionic component, wa is the weight fraction of trifluoroethyl methacrylate, and w_B is the weight fraction of the zwitterionic component.

2.3.4. Differential Fast Scanning Calorimetry. To measure the thermal properties of PT:SBB2VP, which degraded before any glass transitions could be observed by TMDSC, we performed differential fast scanning chip-based calorimetry. 50,51 Measurements were obtained

using the Mettler Toledo Flash DSC1. The empty sensor chip was conditioned according to the manufacturer's procedure four or five times. The temperature of the ceramic support was set at 173 K (-100)°C). Scans were performed under an inert atmosphere of nitrogen with flow rate of about 50 mL/min. PT:SBB2VP copolymer was dissolved in TFE to form a 15% (w/v) solution. Ten droplets of the copolymer solution were deposited onto a clean glass slide using a Headway Research grade spin coater. The slide was spun at 2000 rpm, and the spin time after deposition of the droplets was 1 min. The resulting film's height was less than 10 μ m. Before putting the copolymer film on the sensor, a small droplet of low viscosity silicon oil was placed on the sample side of the sensor using a fine wire to improve thermal contact. Then, small flakes of copolymer film with lateral dimensions of less than 200 μ m were cut, lifted from the glass slide, and mounted on the sample side of the chip sensor of the Flash DSC1 on top of the silicon oil. The copolymer film was heated and cooled several times at 2000 or 1000 K/s from 173 K ($-100~^{\circ}$ C) to temperatures ranging from 593 to 673 K (320 to 400 °C) for observation of any thermal events such as the glass transition or

2.4. Preparation of Thin Film Composite (TFC) Membranes. PT:SBMA, PT:MPC, PT:SB2VP, and PT:SBB2VP copolymers were dissolved in TFE to form 10% (w/v), 12% (w/v), 15% (w/v), and 15% (w/v) solutions, respectively. Upon dissolution, copolymer solution was passed through a 1 μ m glass fiber syringe filter (Whatman) and degassed by placing the sealed vial in an oven at 50 °C for at least an hour until no bubbles were visible to the naked eye. After bringing the solution to room temperature, thin film composite membranes were prepared by coating copolymer solutions onto PVDF 400R ultrafiltration membranes (Nanostone Water, Eden Prairie, MN) using a doctor blade set at a gate size of 25 μ m. Membranes with PT:SBMA and PT:SB2VP copolymer selective layers were immersed immediately in an isopropanol bath for 20 min, while membranes with PT:MPC and PT:SBB2VP were air-dried for 10 min before isopropanol immersion. After the IPA step, all membranes were placed in deionized water for at least 4 h.

2.5. Characterization of Membrane Morphology. 2.5.1. Scanning Electron Microscopy (SEM). To characterize selective layer thickness and morphology, we used SEM. Images were obtained using a Phenom G2 Pure Tabletop SEM operated at 5 kV. Membrane samples were dabbed on a paper towel to remove excess water. Samples were then freeze-fractured using liquid nitrogen and sputter coated with gold-palladium before cross-sectional examination with the SEM.

2.5.2. Fourier Transform Infrared (FTIR) Spectroscopy. To confirm the presence of zwitterionic copolymer selective layers on the TFC membranes, we characterized the chemical structure of the copolymer coatings using attenuated total reflection FTIR (ATR-FTIR) spectroscopy. FTIR spectra were obtained using a JASCO FT/IR-6200 type A spectrometer in absorption mode with a triglycine sulfate (TGS) detector. Membrane samples, 1 cm² in area, were air-dried overnight prior to FTIR analysis. Baseline-corrected spectra were collected over a range of 600-4000 cm⁻¹ at 4 cm⁻¹ resolution and averaged over 128 scans to improve the signal-to-noise ratio. Spectra were processed using the Spectra Manager II software (JASCO).

2.5.3. Contact Angle. To characterize membrane hydrophilicity, we performed contact angle experiments using a goniometer (Ramé-hart 250-F1, Ramé-hart Instrument Co.). Sessile drop contact angle measurements were performed on TFC membranes with selective layers made of PT:SBMA, PT:MPC, PT:SB2VP, and PT:SBB2VP copolymers. Uncoated PVDF 400R ultrafiltration membrane was used as a control. Two types of contact angle measurements were performed on all samples: water-in-air and air-in-water (captive bubble). For water-in-air contact angles, we used air-dried and freezedried samples. To prepare air-dried samples, membranes were dried overnight at room temperature and analyzed the next day. Freezedried samples were prepared by affixing membranes to a rectangular piece cut out of a hexagonal antistatic polystyrene weighing dish using double-sided tape, freeze-drying by dipping in liquid nitrogen for 5 min, followed by lyophilizing for 24 h and analysis immediately after

removal from the lyophilizer. Sessile drop measurements were performed by dropping 2 µL of deionized water droplets onto each sample. Five sessile drop measurements were made immediately after each droplet was placed on the membrane, and the average values are reported. Contact angle analysis was performed using Ramé-hart DROPimage Advanced version 2.4.05.

For captive bubble measurements, a transparent rectangular plastic environmental chamber was placed on the sample stage and filled completely with deionized water. Wet membrane samples were affixed to a glass slide using double-sided tape and placed upside down in the chamber with the membrane completely immersed in water and the sample edges barely supported by small plastic caps. An inverted needle was used to introduce 2 μ L of air bubbles to the sample. Five measurements were made for each sample, and the average values are reported. Contact angle analysis was performed using ImageJ software (Drop Analysis LB-ADSA plugin).

2.6. Characterization of Membrane Performance. To measure membrane performance, filtration experiments were performed on 25 mm diameter membranes using a 10 mL Amicon 8010 stirred deadend filtration cell (Millipore) with an effective filtration area of 4.1 cm². The cells were continuously stirred using a stir plate to minimize concentration polarization and were attached to a 1 gallon reservoir. Flux measurements were performed at a constant pressure of 20 psi (1.4 bar). Deionized water was passed through the membranes until the flux remained stable over at least half an hour. Permeate weight was measured by a Scout Pro SP401 balance connected to a Dell laptop, which automatically takes measurements every 30 s using TWedge 2.4 software (TEC-IT, Austria). Due to the nature of the experiment where flow occurs one droplet at a time, the measured volume can vary by 1-2 droplets (0.05-0.1 mL) at each collected data

Flux is defined as the flow rate through the membrane normalized by membrane area. Permeance is a membrane property that normalizes the flux to account for operating conditions and is

$$L_{\rm p} = \frac{J}{\Delta p} = \frac{1}{R_{\rm total}} \tag{2}$$

where $L_{\rm p}$ is the permeance of the membrane (Lm²⁻ h⁻¹bar⁻¹), J is the water flux across the membrane (Lm⁻² h⁻¹), Δp is the transmembrane pressure (bar), and $R_{\rm total}$ is the total resistance of the TFC membrane to flow (L⁻¹ m² h bar). To account for the hydraulic resistance posed by the support membrane, the resistances-in-series model was used. Having obtained the permeance of the thin film composite membrane, we calculated the total resistance to flow using eq 2. The permeance of the uncoated PVDF 400R base membrane was measured to be 220 \pm 10 Lm⁻² h⁻¹ bar⁻¹. The resistance provided by the uncoated membrane was calculated by taking the inverse of its permeance. The copolymer coating resistance was obtained using

$$R_{\text{coating}} = R_{\text{total}} - R_{\text{support}} \tag{3}$$

where R_{support} is the resistance of the uncoated support membrane (L⁻¹ m^2 h bar) and $R_{coating}$ is the resistance of the copolymer coating (L⁻¹ m² h bar). Finally, copolymer permeability was calculated from the coating resistance and coating thickness, defined as

$$P_{\rm m} = L_{\rm p} \delta = \frac{\delta}{R_{\rm coating}} \tag{4}$$

where $P_{\rm m}$ is copolymer permeability (L μ m m⁻² h⁻¹ bar⁻¹) and δ is the membrane thickness (μ m). For each copolymer, at least four membrane samples from the same sheet were tested. The average values are reported.

To characterize membrane selectivity, we filtered a series of dyes of various sizes by applying a pressure difference of 20 psi (1.4 bar). Aqueous dye solutions (100 mg/L) were passed through the membrane. The first milliliter of filtrate was discarded, and the following milliliter of filtrate was used to calculate rejection by measuring the percentage change in concentration of the feed and the permeate, defined as

$$R = \frac{100(C_{\rm f} - C_{\rm p})}{C_{\rm f}} \tag{5}$$

where R is the solute rejection (%), C_f is feed concentration (mg/L), and C_p is the permeate concentration (mg/L). Dye concentrations of the feed and permeate were measured by UV-vis spectroscopy (Thermo Scientific Genesys 10S). Permeate solutions with dye concentrations above 20 mg/L were diluted to one-tenth of their initial concentration to ensure the linearity of the absorbanceconcentration values. For each copolymer, at least two samples from the same sheet were tested, and the average dye rejection values are reported.

To characterize membrane fouling, filtration experiments were performed using the same equipment and setup. Because the copolymer membranes were found to have quite different permeabilities, tests were performed under constant initial flux conditions to keep the hydrodynamic conditions the same. All membranes were compacted at a transmembrane pressure of 40 psi (2.8 bar). The flux and permeance data thus obtained were used to calculate the pressure needed for the target initial flux, which was kept the same for each membrane. All experiments were performed at a constant initial water flux of 2.2 L m⁻² hr⁻¹, which corresponds to pressures of 7.3, 8.0, 17.4, and 23.8 psi, respectively, for PT:SBMA, PT:MPC, PT:SB2VP, and PT:SBB2VP TFC membranes and 18.5 psi for the commercial poly(ether sulfone) 1 kDa membrane (Sartorius) used as a control. First, deionized water was passed through the membrane until flux stabilized over at least 30 min. Next, the cell and reservoir were emptied and filled with a model protein foulant, 1 g/L BSA in 0.01 M PBS solution (pH 7.4). After filtering the protein solution for 24 h, the cell was rinsed several times with DI water. Thereafter, the cell and reservoir were filled with deionized water to determine the reversibility of fouling. Protein concentration in feed and permeate was quantified using UV absorbance at 280 nm.

3. RESULTS AND DISCUSSION

3.1. Synthesis of Amphiphilic Zwitterionic Copolymers. We synthesized random/statistical copolymers of TFEMA, a hydrophobic monomer, with four zwitterionic monomers using free radical polymerization (FRP). While PTFEMA-r-SBMA was synthesized in our previous study, no other random zwitterionic copolymers of PTFEMA had been previously reported or tested for membrane applications. The four zwitterions were selected to systematically investigate the effect of varying the chemical structure on (1) zwitterion type (sulfobetaine vs phosphorylcholine), (2) chain length between the charges of the zwitterionic monomer (spacer length), and (3) chain length from the C-C backbone to the first charged functional group (linker).

Two of the zwitterionic monomers, SBMA and MPC, were available commercially, and two, SB2VP and SBB2VP, were custom synthesized. Sulfobetaine and phosphorylcholine functional groups were selected (Figure 1) because they are zwitterionic over the entire pH range. The first zwitterionic monomer selected, SBMA, was used in our previous study²⁸ and has an aliphatic quaternary ammonium as the cation and a sulfonate group as the anion. MPC belongs to the phosphorylcholine family with a quaternary ammonium cation but a different anion, a phosphate group. To vary the linker (the groups that connect the polymer backbone to the first charged functional group), we synthesized SB2VP, a sulfobetaine with pyridinium (aromatic quaternary ammonium) as the cation, keeping the same spacer length (three methylene units) and same anion (sulfonate). To vary the spacer length (distance between the charges), another monomer with four methylene groups between the charges was synthesized, called SBB2VP. SB2VP and SBB2VP monomers were synthesized

Table 1. Composition and Glass Transition Temperatures of Homopolymers and Amphiphilic Zwitterionic Copolymers Used in This Study

polymer	zwitterionic monomer content in reaction mixture (wt %)	zwitterionic monomer content in polymer (wt %)	polymer yield (%)	experimental T_g^a (°C)	calculated T_g^b (°C)
PTFEMA	0	0	70	84	N/A
PMPC	100	100	60	175	N/A
PSBMA	100	100	60	220	N/A
PSB2VP	100	100	50	250 ^c	N/A
PSBB2VP	100	100	30	225	N/A
PT:MPC	30	33	60	128	103.4
PT:SBMA	40	36	70	173	108
PT:SB2VP	50	33	60	189	107.6
PT:SBB2VP	50	34	30	82 ^d	106.7

^aDetermined by DSC. ^bCalculated using the Fox equation. ^cThis was difficult to determine accurately as it degrades close to its T_g. ^dDetermined by flash DSC. The T_g expected at higher temperatures was difficult to determine due to polymer degradation.

using modified versions of previously reported procedures 46,47 with yields of 70 and 60% respectively. Zwitterionic amphiphilic copolymers containing 33-36 wt % zwitterionic repeat units were synthesized for this study (Table 1).

PT:MPC copolymers with zwitterionic monomer contents ranging between 30 and 50 wt % were synthesized to screen the properties of this copolymer. At MPC contents greater than 40%, the copolymer would swell extensively in water and show partial or complete solubility. Therefore, the PT:MPC copolymer with an MPC content of 33 wt % was selected for this study. All other copolymers were synthesized and selected to have comparable zwitterionic monomer contents. PT:SBMA with an SBMA content of 36 wt % was synthesized and used in this study. PT:SB2VP and PT:SBB2VP copolymers with similar zwitterionic monomer contents were also synthesized. All copolymers were white, glassy, and soluble fully in TFE and partially in DMSO. Copolymer compositions were determined using ¹H NMR spectroscopy (Bruker Avance III 500 MHz) using 1% LiCl in deuterated DMSO.

PT:SBMA and PT:MPC copolymer compositions were within ~5% of total monomer composition in the reaction mixture, indicating that the copolymerization was essentially random.⁵² Although we tested only one monomer ratio for PT:SB2VP and PT:SBB2VP copolymers, the fact that the zwitterionic monomer is not highly enriched in the copolymers indicates that large zwitterionic blocks are not likely to be present. Although these copolymers would most accurately be described as statistical copolymers whose repeat unit sequence and final composition are determined by monomer reactivity ratios, they will be referred to as random copolymers henceforth to keep the terminology consistent with published literature.

3.2. Characterization of Molecular Weight. Molecular weights were characterized by DLS using 1 mg/mL copolymer solutions in TFE. PT:MPC, PT:SBMA, PT:SB2VP, and PT:SBB2VP copolymers had effective hydrodynamic radii of 32.8 ± 0.5 , 30.3 ± 0.5 , 31.6 ± 1 , and 32.1 ± 0.9 nm, respectively, which corresponded to molecular weights of 1.34 \times 10⁶, 1.19 \times 10⁶, 1.27 \times 10⁶, and 1.3 \times 10⁶ g/mol, respectively, calculated by the software Brookhaven Particle Solutions v. 2.5 based on an internal database of standards. The large relative molecular weights indicate that the copolymers are long chains, likely above the entanglement molecular

3.3. Characterization of Copolymer Self-Assembly. 3.3.1. DSC. While the incompatibility between the fluorinated TFEMA segments and highly polar zwitterionic repeat units may drive microphase separation, the short segment length found in random copolymers may prevent such self-assembly. The self-assembly or thermal properties of these materials has not been previously documented. Microphase separation in these zwitterionic copolymers was first characterized using thermal analysis to determine the glass transition temperature (T_{σ}) value(s) observed in each copolymer using temperature modulated DSC (TMDSC). A microphase separated copolymer is expected to exhibit separate $T_{\rm g}$ values for each domain, whereas a copolymer whose repeat units form a single phase exhibits a T_g value between the T_g s corresponding to the homopolymers of each monomer, predicted by the Fox equation (eq 1). Thus, thermal analysis can give insights into the self-assembly of these copolymers.

Table 1 shows the T_g values obtained from reversible heat flow versus temperature plot for all four copolymers PT:SBMA, PT:MPC, PT:SB2VP, and PT:SBB2VP (see Supporting Information). Reversible heat flow was chosen as it provides useful information about transitions that involve a change in heat capacity (especially glass transition (T_g)) while minimizing kinetic effects, which can play a significant role in small-scale or nanoscale phase separation. T_{gs} of homopolymers corresponding to all five monomers were also measured using TMDSC (Table 1).

The $T_{\rm g}$ of PTFEMA was measured to be 84 °C, comparable with literature reports.⁵⁴ All 4 zwitterionic homopolymers showed very high $T_{\rm g}$ values between 175 and 250 °C, as expected from the very strong dipole-dipole interactions between repeat units. The $T_{\rm g}$ values measured for PSBMA and PSB2VP were consistent with previously published values in the literature. SS PSB2VP and PSBB2VP show higher T_g s due to the pyridine ring, which increases the rigidity of both the backbone and the side groups. The sulfobetaines (PSB2VP, PSBB2VP, and PSBMA) degrade close to their glass transition temperatures.⁵⁵ While both PMPC and PSBMA are esters, the presence of a longer flexible linker group in PMPC allows greater chain mobility, resulting in a lower T_g .

Only a single glass transition was observed for PT:MPC, PT:SBMA, and PT:SB2VP copolymers. No glass transition was observed at temperatures around the homopolymer $T_{\rm g}$ of PTFEMA (~84 °C) in these TMDSC experiments. However, the T_g s observed are much higher than mixed phase T_g values predicted by the Fox equation for these copolymer compositions but lower than the $T_{\rm g}$ of zwitterionic homopolymers (Table 1). This indicates that the observed T_g

ACS Applied Materials & Interfaces

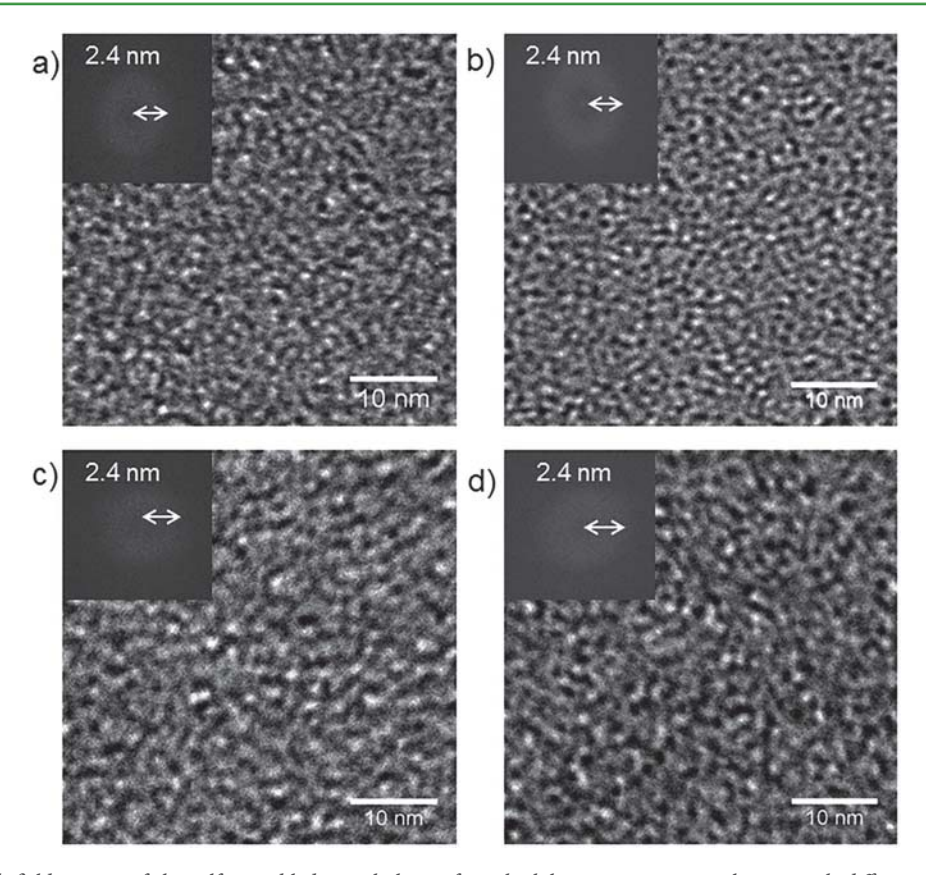


Figure 2. TEM brightfield images of the self-assembled morphology of amphiphilic zwitterionic copolymers with different zwitterionic chemical structures but similar zwitterionic monomer content, exhibiting bicontinuous networks of zwitterionic (dark) and TFEMA (light) microphases. The insets show FFT of the images with the characteristic period shown on the arrow. All four copolymers (a) PT:SBAMA, (b) PT:MPC, (c) PT:SB2VP, and (d) PT:SBB2VP exhibit similar characteristic periods of ~2.4 nm, yielding a zwitterionic channel size around 1.2 nm.

corresponds to a phase that is richer in the zwitterionic monomers than bulk, thus implying a separate, PTFEMA-rich phase. The zwitterionic microphase contains some TFEMA segments that plasticize it, likely due to the fact that the repeat units cannot separate completely due to the random sequence of repeat units along the copolymer backbone.

The data further implies that TFEMA-rich domains must exist in the material. Yet, this $T_{\rm gr}$ expected around 80 °C, was not measurable in these experiments. For a phase-separated copolymer, the lack of observation of two separate glass transition temperatures may arise due to the content of one of the phases being too low to show up on the DSC trace⁵⁶ or to chain confinement effects. ^{57,58} The former explanation is unlikely in this case given the large mass fraction of TFEMA in the copolymer. The PTFEMA segments are confined to very small nanodomains bordered by glassy, rigid zwitterionic monomer domains that limit chain mobility. This may lead to the prevention of chain motion until the confining zwitterionic domains reach their own $T_{\rm g}$ at a much higher temperature. Alternatively, it may simply lead to a very broad, hard to observe T_{σ} . This likely prevented the observation of a T_g for PTFEMA (or PTFEMA-rich) domains in these experiments.

No $T_{\rm g}$ information could be obtained for PT:SBB2VP using TMDSC experiments because the copolymers degraded before a measurable glass transition was reached. To document if microphase separation is expected in this copolymer using thermal analysis, fast scanning calorimetry was used. This

method uses very high heating and cooling rates, which may enable the observation of sharper $T_{\rm g}$ transitions. Fast scanning rates reduce the time spent at high temperature, thereby minimizing the degradation that normally would occur when using the slow scanning rates of TMDSC. Fast scanning thus enables observation of thermal transitions which occur close to the polymer degradation temperature, as shown recently for silk fibroin protein. Sp,60 Flash DSC thermograms of PT:SBB2VP exhibited a $T_{\rm g}$ transition at around 82 °C, as expected for the PTFEMA-rich domains. The $T_{\rm g}$ for the zwitterionic domains was not observed before the onset of polymer degradation, as was the case for the PSBB2VP homopolymer. However, these data confirm the presence of two separate microphases in the PT:SBB2VP copolymer.

3.3.2. TEM. We used TEM to characterize the self-assembled morphology of these amphiphilic zwitterionic copolymers. To obtain contrast, zwitterionic domains were preferentially stained by immersion in 2% aqueous CuCl₂ solution, taking advantage of stable complexes formed between copper and zwitterions. Figure 2 shows brightfield TEM images of PT:SBMA (36 wt %), PT:MPC (33 wt %), PT:SB2VP (33 wt %), and PT:SBB2VP (34 wt %) copolymers. The stained zwitterionic domains of PT:SBMA, PT:SB2VP, PT:SB2VP, and PT:MPC copolymers, appearing dark, were measured to be 34, 32, 32, and 31% of the total area, respectively, using ImageJ software. This is consistent with the copolymer compositions. All copolymers show bicontinuous networks of nanoscale domains of both TFEMA and the zwitterionic component. The

structure is not ordered/periodic, but exhibits a consistent domain size on the order of 1 nm. This morphology is similar to that observed for other random/statistical copolymers with repeat units of highly mismatched polarity such as Nafion.⁶¹ The bicontinuous network of zwitterionic, hydrophilic repeat units can act as effective channels for the passage of water. This is similar to hydration and ion conduction in Nafion that occurs through the ~1 nm domains where the charged groups in the polymer aggregate. 62 Interestingly, we did not see a measurable change in zwitterionic domain sizes by varying the zwitterionic component in the copolymer. All copolymer films exhibit a domain periodicity of ~2.4 nm/cycle determined from the FFT of the images, which corresponds to characteristic zwitterionic domain sizes of ~1.2 nm. These results indicate that the chemical structure of the zwitterionic group does not have a significant effect on the zwitterionic domain size.

3.4. Preparation and Characterization of TFC Membranes. 3.4.1. Membrane Manufacture and Morphology. We prepared thin film composite membranes by coating copolymer solutions in TFE onto commercially available ultrafiltration (UF) support membranes using a doctor blade, followed by solvent evaporation for 0-10 min and immersion in an isopropanol bath to precipitate the copolymer. Isopropanol is a nonsolvent for the copolymer, so the copolymer coagulates on the porous membrane surface upon immersion into the isopropanol bath. This led to faster membrane formation compared with solvent evaporation and also prevented the penetration of the copolymer solution into the internal pores of the support membrane through capillary forces. This approach can be used to form dense or porous layers depending on the diffusivities and solvent qualities of the solvent and nonsolvent.⁵ Indeed, for PT:MPC and PT:SBB2VP TFC membranes, direct immersion in IPA led to 5-10 μm thick porous coatings initially, as observed under SEM (see Supporting Information). Air drying membranes for 10 min before isopropanol immersion allowed some solvent to leave, thereby increasing the local polymer concentration at the surface before solvent/nonsolvent exchange occurs. This allowed the production of dense coatings for PT:MPC and PT:SBB2VP with no visible pores under SEM despite faster copolymer precipitation. No drying time was necessary for PT:SBMA and PT:SB2VP TFC membranes. The resultant TFC membranes had dense copolymer selective layers $\sim 1-1.2$ μ m in thickness, as confirmed by SEM (Figure 3).

3.4.2. FTIR Spectroscopy. To confirm the presence and chemistry of the selective layer, we performed ATR-FTIR spectroscopy measurements on the TFC membrane surface. Figure 4 shows the ATR-FTIR spectra of the uncoated support membrane and the TFC zwitterionic copolymer selective layers. Each copolymer exhibits several FTIR peaks that are not present in the PVDF spectrum, confirming the presence of the selective layer and the retention of the copolymer chemical structure. Ester groups, present in TFEMA, lead to peaks at $1740 \text{ cm}^{-1} \text{ (C=O)}$ and $1170 \text{ cm}^{-1} \text{ (C-O)}$. The intensity of these peaks is higher in PT:SBMA and PT:MPC due to the ester groups of the zwitterionic component. PT:SBMA and PT:MPC show a peak at 1480 cm⁻¹, characteristic of aliphatic quaternary ammonium groups.³⁴ The FTIR spectrum of PT:MPC shows two additional peaks at 1086 and 1235 cm⁻¹ that represent (OPOCH2) and (POCH2) groups present in MPC.⁶⁴ Sulfobetaine groups in PT:SBMA, PT:SB2VP, and PT:SBB2VP lead to peaks at 1036 and 1201 cm⁻¹ due to symmetric and asymmetric stretching of the SO₃⁻ group. 43

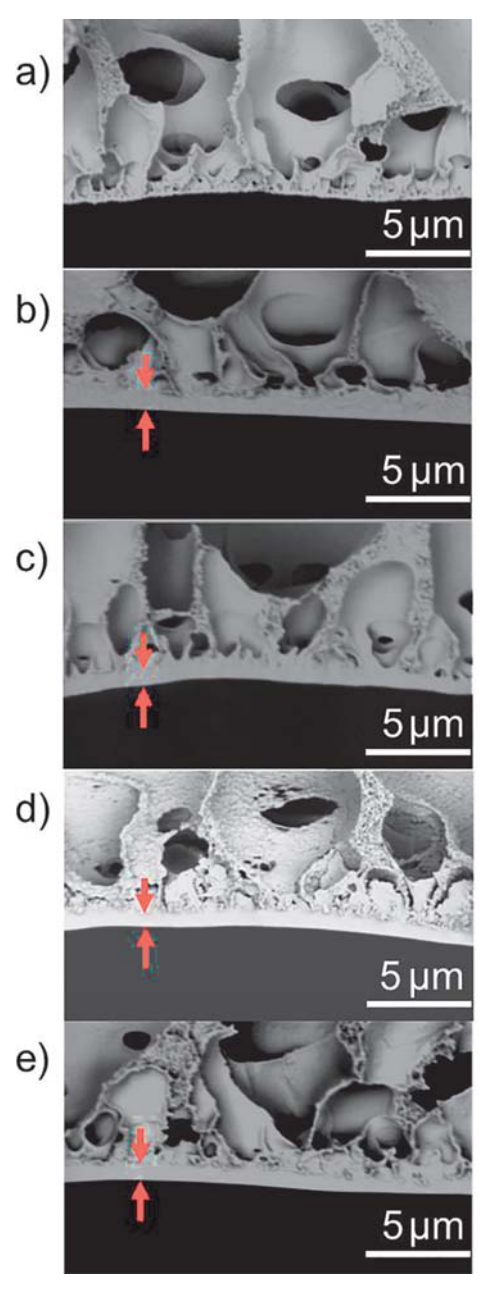
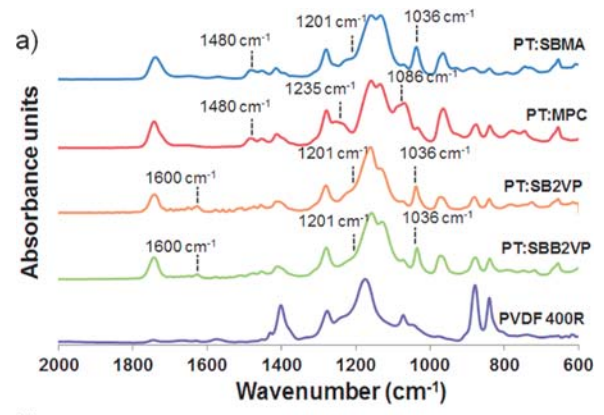


Figure 3. Cross-sectional SEM images of uncoated support membrane and TFC membranes with selective layers made of amphiphilic zwitterionic copolymers. (a) Uncoated support membrane (PVDF 400R), (b) PT:SBMA, (c) PT:MPC, (d) PT:SB2VP, and (e) PT:SBB2VP. All four TFC membranes show a dense $\sim\!1~\mu\mathrm{m}$ copolymer coating as indicated by arrows (10 000× magnification).

PT:SB2VP and PT:SBB2VP exhibit a peak at $\sim\!1600$ cm $^{-1}$, characteristic of the C–C and C–N stretching vibrations in the pyridine ring. 65

3.4.3. Contact Angle. To characterize the surface hydrophilicity of TFC membranes coated with zwitterionic copolymer selective layers, we performed contact angle experiments. Sessile drop contact angle measurements were performed on air-dried and freeze-dried TFC membranes. Captive air bubble contact angle measurements were also performed on wet membrane samples for each TFC membrane (Figure 4).



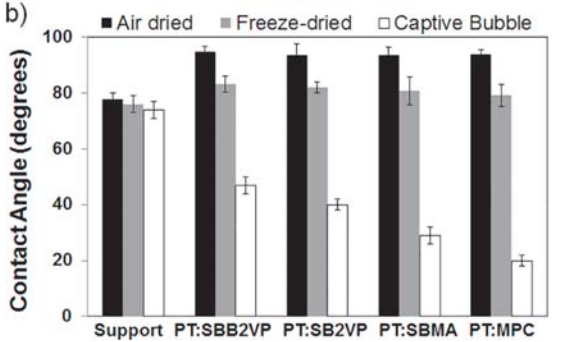


Figure 4. Surface chemical properties of the uncoated support membrane and TFC membranes with selective layers made of PT:SBB2VP, PT:SB2VP, PT:SBMA, and PT:MPC copolymers. (a) ATR-FTIR spectra. (b) Sessile drop contact angle measurements performed on air-dried (black) and freeze-dried (gray) samples and captive air bubble contact angle measurements (white). Error bars indicate standard deviation of five measurements on each sample.

No significant difference in contact angle between the various TFC membranes was observed in sessile drop measurements performed on air-dried membranes (Figure 4b). All TFC membranes exhibited contact angles above 90° and higher than that of the base membrane, which indicates that the surface was hydrophobic. This contact angle is in the range typically found for fluorinated polymers⁶⁶ and suggests that in the dry state, to minimize surface energy, zwitterionic groups orient away from the surface exposed to air. This leaves the surface covered mainly by hydrophobic trifluoroethyl groups present in TFEMA. This can occur due to the rearrangement of functional groups as the membrane is dried for analysis. However, membranes are immersed in water during use.

To minimize surface reorganization and preserve the surface chemistry in effect during membrane use, we freeze-dried the samples in a lyophilizer for 24 h and analyzed the samples immediately after. Contact angles were lower, around $\sim 80^{\circ}$ (Figure 4), but no significant change across different zwitterionic copolymer TFC membrane samples was observed. The fact that these surfaces are still very hydrophobic despite the presence of highly hydrophilic zwitterionic groups in the copolymer implies that freeze-drying was only partially successful in preventing surface reorganization.

Captive air bubble contact angle is a useful surface analysis technique where an air bubble is introduced while the sample is kept immersed in a liquid (usually water).⁶⁷ This maintains the membrane surface fully hydrated during the experiment and closely mimics the conditions under which membranes operate. Using the captive air bubble method, significantly lower contact angles of 20 \pm 2, 29 \pm 3, 40 \pm 2, and 47 \pm 3° were obtained for membranes coated with PT:MPC, PT:SBMA, PT:SB2VP, and PT:SBB2VP copolymers, respectively. These observed differences in wettability are attributed to an increase in hydrophilicity in the order: PT:SBB2VP < PT:SB2VP < PT:SBMA < PT:MPC. These results imply that phosphorylcholine is more hydrophilic than the sulfobetaines. In addition, zwitterionic copolymer membranes with ester-based sulfobetaines are more hydrophilic than pyridinium-based sulfobetaines. The change in wettability from air-dried/freeze-dried samples to wet samples supports our hypothesis that surface reorganization of groups on the membrane surface was dominant in the dry state when membranes were exposed to air. The contact angle of uncoated commercial PDVF 400R UF support membrane is $78 \pm 4^{\circ}$, comparable with sessile drop contact angles.

3.5. Characterization of Membrane Performance. 3.5.1. Water Permeability. Membranes with selective layers made of PT:SBMA, PT:MPC, PT:SB2VP, and PT:SBB2VP exhibited pure water permeances that ranged between 1.4 ± 0.3 and 5.83 ± 1 L m⁻² h⁻¹ bar⁻¹ (Table 2). These values were comparable to or even higher than those of a commercial PES membrane with a reported nominal molecular weight cutoff (MWCO) of 1 kDa (Sartorius), which had a water permeance of 2.5 ± 0.1 L m⁻² h⁻¹ bar⁻¹. This membrane was selected as its size cutoff was comparable with that of PT:SBMA membranes as documented in previous studies.²⁸

The permeances of PT:MPC-coated and PT:SBMA-coated membranes were much higher than the permeances obtained for PT:SB2VP- and PT:SBB2VP-coated membranes.

Water permeance of TFC membranes is strongly dependent on membrane thickness. Most RO and NF membranes have thin selective layers ${\sim}0.1~\mu{\rm m}$ in thickness, whereas the selective layers of membranes reported here were ${\sim}1{-}1.2~\mu{\rm m}$ thick. To account for differences that arise from variations in coating thickness, we calculated water permeabilities of the copolymers

Table 2. Surface Chemistry Properties and Performance of TFC Membranes with Zwitterionic Copolymer Selective Layers in Comparison to a Commercial Membrane of Similar Pore Size

membrane coating material	permeance (L m ⁻² hr ⁻¹ bar ⁻¹)	coating thickness (μm)	permeability a (L μ m m $^{-2}$ hr $^{-1}$ bar $^{-1}$)	water uptake ^b (%)	water contact angle ^c (deg)	irreversible flux $loss^d$ (%)
PT:MPC	4.74 ± 0.8	1.2 ± 0.2	5.9 ± 0.8	25	20 ± 2	<1
PT:SBMA	5.83 ± 1	1.0 ± 0.2	6.1 ± 1	22	29 ± 3	<1
PT:SB2VP	2.2 ± 0.4	1.0 ± 0.2	2.2 ± 0.2	11	40 ± 2	8
PT:SBB2VP	1.4 ± 0.3	0.86 ± 0.2	1.2 ± 0.3	8	47 ± 3	16
PES 1 kDa	2.5 ± 0.1	N/A	N/A	N/A	N/A	50

^aCalculated using resistance in series model. ^bSolvent-cast polymer films soaked in water for 24 h. ^cMeasured using the captive bubble method. ^dDetermined after 24 h protein filtration.

using the resistances in series model described in eqs 3 and 4 (Table 2). Permeabilities of PT:MPC and PT:SBMA selective layers are comparable and about three times higher than the permeabilities of PT:SB2VP and PT:SBB2VP selective layers. In comparison, selective layer permeabilities of common RO and NF membranes are in the range 0.047-0.28 and 0.3-1.8 L μm m⁻² h⁻¹ bar⁻¹, respectively.⁶⁸ Hence, PT:MPC and PT:SBMA selective layers exhibit permeabilities significantly higher than those of commercial NF and RO selective layers, while permeabilities of PT:SB2VP and PT:SBB2VP selective layers are comparable to those of commercial NF and RO selective layers. By optimizing membrane coating conditions to reduce the selective layer thickness, even higher permeances can be achieved.

The differences between the selective layer permeabilities for different zwitterionic copolymers may arise from differences in volume fraction or size of channels, tortuosity, or hydrophilicity. As indicated by the TEM results, all four copolymers led to membranes with similar channel size, volume fraction, and morphology. Thus, the observed differences in permeability are due to the relative hydrophilicities and hydration of the zwitterionic copolymers used as selective layers. The trends in copolymer permeability are in agreement with the contact angle measurements performed by captive bubble technique. These results are also supported by the water uptake by copolymer films measured by immersing solvent-cast films in deionized water for 24 h. PT:SBMA and PT:MPC took up significantly larger amounts of water than PT:SB2VP and PT:SBB2VP copolymers (Table 2). These results suggest that the relative hydrophobicity of the zwitterions in PT:SB2VP and PT:SBB2VP limits the hydration of the zwitterionic domains and leads to lower permeability in comparison with PT:SBMA and PT:MPC, which feature more hydrophilic zwitterions.

3.5.2. Membrane Selectivity. To probe membrane selectivity, we filtered a series of dyes of various sizes through our membranes. We selected dyes with rigid chemical structures whose sizes are comparable to the zwitterionic domain size measured by TEM. Dye diameters were estimated using Molecular Modeling Pro (ChemSW) by determining the molecular volume of the solute and calculating the diameter of a sphere of equivalent volume. 28,53,69,70 Previous work on PT:SBMA membranes has shown that this family of materials perform size-based separations, with neutral solutes fitting on the same rejection curve as anionic solutes.²⁸ Anionic dyes were used in this study for the sake of simplicity. Figure 5 shows the rejection of these dyes through PT:SBMA, PT:MPC, PT:SB2VP, and PT:SBB2VP TFC membranes. These membranes exhibit sharp, size-based selectivity with an effective size cutoff around 0.8-1 nm. The size cutoff is likely a slight underestimate as the software used to determine dye diameters does not take into account solute geometry or the hydration shell around the dyes. Furthermore, the channels are partially filled with the zwitterionic groups. This can reduce the effective channel size in filtration in comparison with that measured by TEM (~1.2 nm). Therefore, there is close agreement between the channel size measured through filtration experiments and that measured with TEM, consistent with our previous results for membranes prepared using PT:SBMA copolymers.²⁸

We did not observe a significant change in effective channel size between TFC membranes made with random copolymers with different zwitterionic groups. While these groups are chemically different, the small changes in their structure do not appear to be sufficient to create significant changes in their

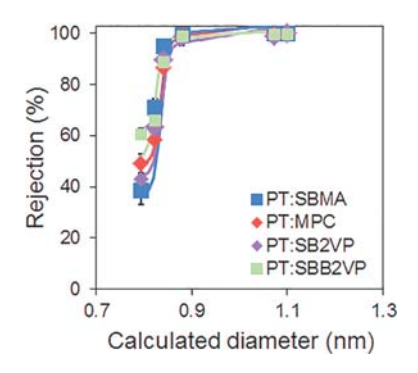


Figure 5. Rejection of anionic dyes by TFC membranes with amphiphilic zwitterionic copolymer selective layers with different zwitterionic chemical structures but similar zwitterionic monomer content, exhibiting sharp size-based selectivity with an effective size cutoff of ~ 1 nm.

interion distance or self-assembled channel size. The distance between the C-C backbone to the first charged functional group was calculated to be 3.6 Å for SB2VP and SBB2VP and 5.2 Å for SBMA and MPC using Molecular Modeling Pro. This ~1.5 Å difference does not lead to a change in channel size, likely because these linkers do not necessarily participate in the formation of the water channels. The spacer connecting the two charges is three units long in SB2VP and four units long in SBB2VP, corresponding to an increase in the spacer length by 0.66 Å in a fully extended conformation. This difference does not seem to be large enough to significantly alter the selectivity of these membranes. Channel size did not vary with the zwitterion chemical structure either, likely due to similar degrees of self-association and electrostatic interactions between the charged groups of the zwitterions used in this study. This is attributed to similarly sized anions (sulfonate and phosphate) and hence similar charge densities between the sulfobetaines and phosphorylcholines.³³ Zwitterions with larger spacer lengths are difficult to synthesize and were thus not prepared for this study. Overall, these results show that zwitterion structure does not significantly affect the effective pore size but has a significant effect on permeability and

3.5.3. Fouling Resistance. Previous research on PT:SBMAcoated TFC membranes showed exceptional fouling resistance to common foulants such as proteins and oil emulsions.²⁸ On the basis of our hypothesis, we expect the TFC membranes with varying zwitterionic chemical structures and hydration properties to exhibit differences in fouling performance that have not been explored before. To compare the performance of these novel amphiphilic zwitterionic copolymer membranes, we performed dead-end stirred cell filtration experiments using BSA as a model foulant because proteins tend to adsorb strongly onto membranes and cause extensive fouling. We filtered 1 g/L BSA in 0.01 M phosphate buffered saline solution (pH 7.4) through these membranes. We measured foulant flux over a 24 h period as well as the water flux before and after filtering the foulant solution (Figure 6). To account for the differences in membrane permeabilities, we performed the tests at a constant initial flux of 2.2 L m⁻² hr⁻¹. BSA rejection was >99% for all membranes, consistent with the large globular size of the protein $(8 \times 3 \text{ nm})$ and the pore size of the membranes.

PT:SBMA and PT:MPC feature different zwitterions with similar ester linkages attaching them to the polymer carbon backbone. These were also the most hydrophilic copolymers, as

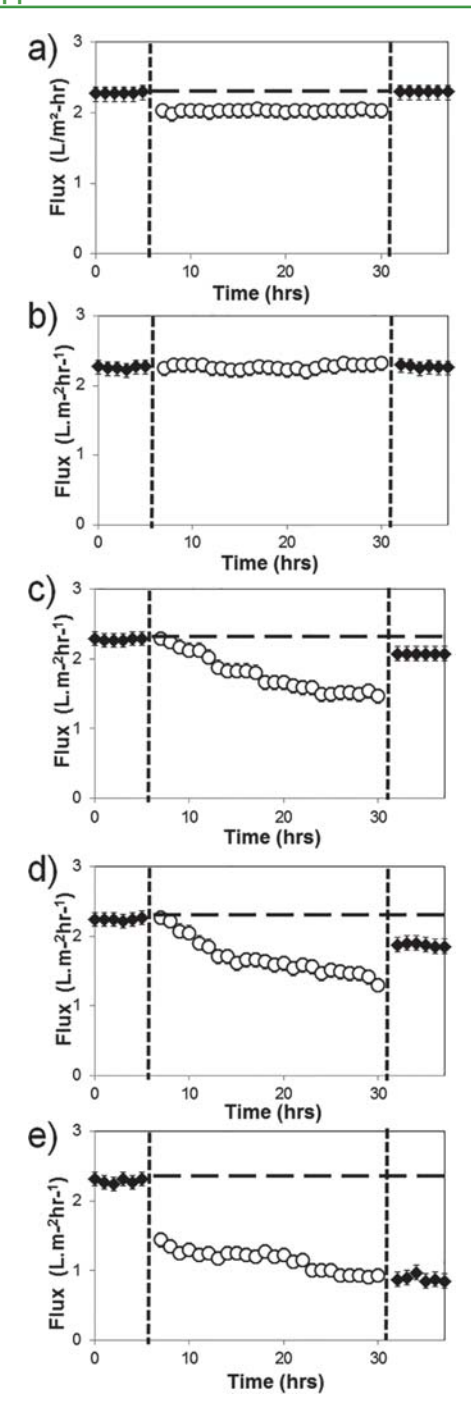


Figure 6. Dead-end filtration of protein solutions through TFC membranes with selective layers made of (a) PT:SBMA, (b) PT:MPC, (c) PT:SB2VP, and (d) PT:SBB2VP copolymers and (e) a commercial membrane of similar pore size, PES 1 kDa (Sartorius). PT:SBMA and PT:MPC TFC membranes showed negligible decline in water flux (black) after protein filtration (white). PT:SB2VP and PT:SBB2VP TFC membranes showed 8 and 16% irreversible flux decline, respectively. The commercial membrane showed 50% irreversible flux loss. Horizontal dotted lines are for visual aid.

indicated by captive bubble contact angle and water uptake measurements. Figures 6a and b show the fouling performance of the TFC membranes when bovine serum albumin is passed through these membranes. PT:SBMA-coated (Figure 6a) and PT:MPC-coated membranes (Figure 6b) show no irreversible

decline in flux after protein filtration. The fluxes before and after protein filtration are all within error margins of each other. In fact, PT:MPC-coated TFC membrane shows no decline in flux even during protein filtration. While the flux is completely recovered after rinsing the membrane with deionized water, PT:SBMA-coated membrane shows some flux decline during protein filtration (<18%). These results indicate the excellent fouling resistance of both PT:MPC and PT:SBMA. This is, to our knowledge, the first time no flux loss was observed during the entire dead-end fouling experiment.

Figures 6c and d show the protein filtration performance of PT:SB2VP-coated and PT:SBB2VP-coated membranes. These two copolymers also have a sulfobetaine zwitterionic group like SBMA, but it is attached to the polymer backbone through a less hydrophilic, pyridine-containing functional group. SBB2VP also has a longer aliphatic spacer between the charged groups. The PT:SB2VP- and PT:SBB2VP-coated membranes exhibit flux declines of 32 and 33%, respectively, during protein filtration, and partial irreversible flux losses of 8 and 16%, respectively, that could not be recovered after rinsing the membrane with deionized water. This indicates that zwitterionic copolymer membranes with ester-based sulfobetaines are more fouling resistant than membranes with pyridinium-based sulfobetaines. This implies that the rigidity and/or hydrophobicity of the linker group can dramatically affect foulantmembrane interactions and fouling resistance performance of the membrane. The higher irreversible flux loss for PT:SBB2VP-coated membrane is attributed to the increased hydrophobicity of the zwitterionic group due to the longer spacer length, which leads to lower hydration and increased protein interactions. This is consistent with the simulations reported in literature for carboxybetaines, which report that as the distance between the charged sites increases, there is more self-association and less hydration.³² It is also reported that sulfobetaines with three methylene groups have hydration lower than that of carboxybetaines with two methylene groups between the charges. These results are in good agreement with the relative hydrophilicities and hydration properties of PT:SBMA, PT:MPC, PT:SB2VP, and PT:SBB2VP TFC membranes observed by contact angle and water uptake measurements.

As a control, we used a commercial membrane with a size cutoff similar to ours, a PES membrane with a reported nominal MWCO of 1 kDa (Sartorius). The water permeance and selectivity of this membrane has been characterized in our previously published paper. It had a water permeance of $2.2 \pm 0.1 \, \mathrm{L} \, \mathrm{m}^{-2} \, \mathrm{h}^{-1} \, \mathrm{bar}^{-1}$ before foulant filtration and exhibited a flux decline of ~50% after protein filtration which was not recovered after a water rinse (Figure 6e). Similar results were obtained when membranes were all tested using a transmembrane pressure of 20 psi, leading to higher fluxes for all membranes except PT:SBB2VP (see Supporting Information). This demonstrates that all four zwitterionic copolymers exhibited much better resistance to fouling than the commercial alternative.

4. CONCLUSIONS

In this work, we investigated the effect of the chemical structure of zwitterionic monomers on the self-assembled morphology, hydrophilicity, water uptake, permeability, and fouling resistance of their random copolymers with a fluorinated monomer. We surveyed four copolymers of a fluorinated monomer with different zwitterionic monomers, three of which have not been

previously reported, by varying the zwitterion type (sulfobetaine and phosphorylcholine), linker group (from the C-C backbone to the first charged functional group), and spacer length (distance between the charged groups). We prepared their copolymers with the hydrophobic monomer TFEMA at similar zwitterionic/hydrophobic monomer ratios and prepared membranes by coating these copolymers on a porous support to form a TFC membrane. These novel membranes exhibit a size-based selectivity with an effective pore size of ~1 nm as demonstrated by filtering anionic dyes, corresponding to an effective MWCO of about 1000 Da.

All four copolymers microphase separated into bicontinuous, disordered network morphologies with zwitterionic and hydrophobic domains ~1.2 nm in size. The zwitterionic domains acted as pathways or channels for the permeation of water and solutes smaller than the domain size. Interestingly, different zwitterionic monomers led to no measurable differences in the microphase separated morphologies or the effective pore/channel sizes.

In contrast, different zwitterionic groups led to different hydrophobicities, hydration properties, and protein interactions. Contact angle and water uptake experiments showed that zwitterionic copolymers with ester-based zwitterions are more hydrophilic than membranes with pyridinium-based zwitterions. The relative hydrophilicity is found to increase in the order PT:SBB2VP < PT:SB2VP < PT:SBMA < PT:MPC. Water permeabilities of PT:MPC and PT:SBMA selective layers were three times higher than those of relatively hydrophobic PT:SB2VP and PT:SBB2VP. There were similar trends in the fouling resistance of these zwitterionic copolymers. After protein filtration, PT:SB2VP and PT:SBB2VP TFC membranes showed some irreversible flux loss (8 and 16%). Both PT:SBMA and PT:MPC TFC membranes exhibited excellent, complete resistance to irreversible fouling in these experiments.

PT:MPC membranes showed no decline in flux throughout the duration of this 24 h, dead-end fouling experiment, even during the filtration of the protein solution. This degree of fouling resistance is, to our knowledge, unprecedented. Membranes typically exhibit at least some flux loss due to the reversible accumulation of foulants on their surface. Combined with their high permeance and sharp selectivity, these membranes are excellent candidates for a range of filtration applications, from peptide drug purification to wastewater

This is, to our knowledge, the first time the microphase separated structures of copolymers with different zwitterionic groups were documented and linked with their performance as membrane selective layers. The structure-property relationships developed here can serve as guidelines to prepare new zwitterionic materials for various applications such as membranes, drug delivery, and sensors.

ASSOCIATED CONTENT

Supporting Information

This material is available free of charge. The Supporting Information is available free of charge on the ACS Publications website at DOI: 10.1021/acsami.7b04884.

Detailed methods, synthesis scheme (free radical polymerization), DSC plots of copolymers used in this study (PT:SBMA, PT:MPC, PT:SB2VP, and PT:SBB2VP), resistance-in-series model equations, information about dyes used, and additional fouling experiments conducted at matching pressures (PDF)

AUTHOR INFORMATION

Corresponding Author

*Phone: 617-627-4681; E-mail: ayse.asatekin@tufts.edu.

Ayse Asatekin: 0000-0002-4704-1542

Funding

This research was supported by Tufts University, the National Science Foundation (NSF) under CBET-1553661, CBET-1437772, CHE-1508049, and DMR-1608125, and the Massachusetts Clean Energy Council (MassCEC) Catalyst Award Grant PV3316.

The authors declare no competing financial interest.

ACKNOWLEDGMENTS

TEM was performed utilizing the W.M. Keck foundation Biological Imaging Facility at the Whitehead Institute. Authors thank Dr. Nicki Watson at the Whitehead Institute for help with TEM data acquisition. Authors also thank David Wilbur, Chiara Vannucci and Akash Mittal for experimental help and useful discussions. Authors thank Prof. Christoph Schick (U. Rostock, Rostock, Germany) for hosting PC during a sabbatical stay and for providing use of the Mettler Flash DSC1.

ABBREVIATIONS

AIBN, azobis(isobutyronitrile) MEHQ, 4-methoxy phenol SBMA, sulfobetaine methacrylate MPC, 2-methacryloyloxyethyl phosphorylcholine SB2VP, sulfobetaine 2-vinylpyridine SBB2VP, sulfobutylbetaine 2-vinylpyridine TFEMA, 2,2,2-trifluoroethyl methacrylate DMSO, dimethyl sulfoxide TFE, trifluoroethanol PES, poly(ether sulfone) PT:MPC, PT:MPC copolymer PT:SBMA, PT:SBMA copolymer PT:SB2VP, PT:SB2VP copolymer PT:SBB2VP, PT:SBB2VP copolymer TFC, thin film composite BSA, bovine serum albumin DSC, differential scanning calorimetry TMDSC, temperature modulated DSC TEM, transmission electron microscopy SEM, scanning electron microscopy MWCO, molecular weight cutoff

REFERENCES

- (1) Ciardelli, G.; Corsi, L.; Marcucci, M. Membrane Separation for Wastewater Reuse in the Textile Industry. Resour., Conserv. Recycl. **2001**, *31*, 189–197.
- (2) Burnouf, T.; Radosevich, M. Nanofiltration of Plasma-Derived Biopharmaceutical Products. Haemophilia 2003, 9 (1), 24-37.
- (3) van Reis, R.; Zydney, A. Membrane Separations in Biotechnology. Curr. Opin. Biotechnol. 2001, 12, 208-211.
- (4) Petersen, R. J. Composite Reverse Osmosis and Nanofiltration Membranes. J. Membr. Sci. 1993, 83, 81-150.
- (5) Baker, R. W. Membrane Technology and Applications; Wiley: Hoboken, NJ, 2012.

- (6) Ostuni, E.; Chapman, R. G.; Holmlin, R. E.; Takayama, S.; Whitesides, G. M. A Survey of Structure-Property Relationships of Surfaces that Resist the Adsorption of Protein. Langmuir 2001, 17 (18), 5605-5620.
- (7) Holmlin, R. E.; Chen, X. X.; Chapman, R. G.; Takayama, S.; Whitesides, G. M. Zwitterionic SAMs that Resist Nonspecific Adsorption of Protein from Aqueous Buffer. Langmuir 2001, 17 (9),
- (8) Luk, Y.-Y.; Kato, M.; Mrksich, M. Self-Assembled Monolayers of Alkanethiolates Presenting Mannitol Groups Are Inert to Protein Adsorption and Cell Attachment. Langmuir 2000, 16, 9604-9608.
- (9) Statz, A. R.; Meagher, R. J.; Barron, A. E.; Messersmith, P. B. New Peptidomimetic Polymers for Antifouling Surfaces. J. Am. Chem. Soc. 2005, 127 (22), 7972-7973.
- (10) Zhang, Z.; Chao, T.; Chen, S. F.; Jiang, S. Y. Superlow Fouling Sulfobetaine and Carboxybetaine Polymers on Glass Slides. Langmuir **2006**, 22 (24), 10072–10077.
- (11) Zhang, Z.; Chen, S. F.; Chang, Y.; Jiang, S. Y. Surface Grafted Sulfobetaine Polymers via Atom Transfer Radical Polymerization as Superlow Fouling Coatings. J. Phys. Chem. B 2006, 110 (22), 10799-
- (12) Kitano, H.; Kawasaki, A.; Kawasaki, H.; Morokoshi, S. Resistance of Zwitterionic Telomers Accumulated on Metal Surfaces Against Nonspecific Adsorption of Proteins. J. Colloid Interface Sci. **2005**, 282 (2), 340–348.
- (13) Sun, Q.; Su, Y. L.; Ma, X. L.; Wang, Y. Q.; Jiang, Z. Y. Improved Antifouling Property of Zwitterionic Ultrafiltration Membrane Composed of Acrylonitrile and Sulfobetaine Copolymer. J. Membr. Sci. 2006, 285 (1-2), 299-305.
- (14) Ladd, J.; Zhang, Z.; Chen, S.; Hower, J. C.; Jiang, S. Zwitterionic Polymers Exhibiting High Resistance to Nonspecific Protein Adsorption from Human Serum and Plasma. Biomacromolecules **2008**, 9 (5), 1357–1361.
- (15) He, Y.; Hower, J.; Chen, S.; Bernards, M. T.; Chang, Y.; Jiang, S. Molecular Simulation Studies of Protein Interactions with Zwitterionic Phosphorylcholine Self-Assembled Monolayers in the Presence of Water. Langmuir 2008, 24, 10358-10364.
- (16) Chen, S.; Zheng, J.; Li, L.; Jiang, S. Strong Resistance of Phosphorylcholine Self-Assembled Monolayers to Protein Adsorption: Insights into Nonfouling Properties of Zwitterionic Materials. J. Am. Chem. Soc. 2005, 127, 14473-14478.
- (17) Holmlin, R. E.; Chen, X.; Chapman, R. G.; Takayama, S.; Whitesides, G. M. Zwitterionic SAMS That Resist Nonspecific Adsorption of Protein from Aqueous Buffer. Langmuir 2001, 17, 2841-2850.
- (18) Ishihara, K.; Nomura, H.; Mihara, T.; Kurita, K.; Iwasaki, Y.; Nakabayashi, N. Why Do Phospholipid Polymers Reduce Protein Adsorption? J. Biomed. Mater. Res. 1998, 39 (2), 323-330.
- (19) Georgiev, G. S.; Kamenska, E. B.; Vassileva, E. D.; Kamenova, I. P.; Georgieva, V. T.; Iliev, S. B.; Ivanov, I. a. Self-Assembly, Antipolyelectrolyte Effect, and Nonbiofouling Properties of Polyzwitterions. Biomacromolecules 2006, 7 (4), 1329-1334.
- (20) Chen, S.; Jiang, S. A New Avenue to Nonfouling Materials. Adv. Mater. 2008, 20 (2), 335-338.
- (21) Wu, J.; Lin, W.; Wang, Z.; Chen, S.; Chang, Y. Investigation of the Hydration of Nonfouling Material Poly(Sulfobetaine Methacrylate) by Low-Field Nuclear Magnetic Resonance. Langmuir 2012, 28 (19), 7436-7441.
- (22) Herzberg, M.; Sweity, A.; Brami, M.; Kaufman, Y.; Freger, V.; Oron, G.; Belfer, S.; Kasher, R. Surface Properties and Reduced Biofouling of Graft-Copolymers that Possess Oppositely Charged Groups. Biomacromolecules 2011, 12 (4), 1169-1177.
- (23) Bredas, J. L.; Chance, R. R.; Silbey, R. Head-Head Interactions in Zwitterionic Associating Polymers. Macromolecules 1988, 21 (6), 1633-1639.
- (24) Ehrmann, M.; Galin, J. C. Statistical n-Butyl Acrylate-Sulfonato-Propylbetaine copolymers: 1. Synthesis and Molecular Characterization. Polymer 1992, 33 (4), 859-865.

- (25) Ehrmann, M.; Mathis, A.; Meurer, B.; Scheer, M.; Galin, J. C. Statistical n-Butyl Acrylate-(Sulfopropy1)ammonium Betaine Copolymers. 2. Structural Studies. Macromolecules 1992, 25, 2253-2261.
- (26) Ehrmann, M.; Muller, R.; Galin, J. C.; Bazuin, C. G. Statistical n-Butyl Acrylate-(Sulfopropy1)ammonium Betaine Copolymers. 4. Dynamic Mechanical Properties. Macromolecules 1993, 26, 4910-
- (27) Ehrmann, M.; Galin, J. C.; Meurer, B. Statistical n-Butyl Acrylate-Sulfopropyl Betaine Copolymers. 3. Domain Size Determination by Solid-state NMR Spectroscopy. Macromolecules 1993, 26, 988-993.
- (28) Bengani, P.; Kou, Y.; Asatekin, A. Zwitterionic Copolymer Self-Assembly for Fouling Resistant, High Flux Membranes with Size-Based Small Molecule Selectivity. J. Membr. Sci. 2015, 493, 755-765.
- (29) Laschewsky, A. Structures and Synthesis of Zwitterionic Polymers. Polymers 2014, 6 (5), 1544-1601.
- (30) Shao, Q.; Jiang, S. Molecular Understanding and Design of Zwitterionic Materials. Adv. Mater. 2015, 27 (1), 15-26.
- (31) Shao, Q.; He, Y.; White, A. D.; Jiang, S. Difference in Hydration between Carboxybetaine and Sulfobetaine. J. Phys. Chem. B 2010, 114, 16625-16631.
- (32) Shao, Q.; Jiang, S. Effect of Carbon Spacer Length on Zwitterionic Carboxybetaines. J. Phys. Chem. B 2013, 117 (5), 1357-
- (33) Shao, Q.; Mi, L.; Han, X.; Bai, T.; Liu, S.; Li, Y.; Jiang, S. Differences in Cationic and Anionic Charge Densities Dictate Zwitterionic Associations and Stimuli Responses. J. Phys. Chem. B 2014, 118 (24), 6956-6962.
- (34) Weers, J. G.; Rathman, J. F.; Axe, F. U.; Crichlow, C. A.; Foland, L. D.; Scheuing, D. R.; Wiersema, R. J.; Zielske, A. G. Effect of the Intramolecular Charge Separation Distance on the Solution Properties of Betaines and Sulfobetaines. Langmuir 1991, 7, 854-867.
- (35) He, Y.; Tsao, H. K.; Jiang, S. Improved Mechanical Properties of Zwitterionic Hydrogels with Hydroxyl Groups. J. Phys. Chem. B 2012, 116 (19), 5766-5770.
- (36) Kathmann, E. E.; White, L. A.; McCormick, C. L. Water Soluble Polymers: 70. Effects of Methylene versus Propylene Spacers in the pH and Electrolyte Responsiveness of Zwitterionic Copolymers Incorporating Carboxybetaine Monomers. Polymer 1997, 38, 879-
- (37) White, A.; Jiang, S. Local and Bulk Hydration of Zwitterionic Glycine and its Analogues through Molecular Simulations. J. Phys. Chem. B 2011, 115, 660-667.
- (38) Shao, Q.; Jiang, S. Influence of Charged Groups on the Properties of Zwitterionic Moieties: A Molecular Simulation Study. J. Phys. Chem. B 2014, 118, 7630-7637.
- (39) Zhang, Z.; Chao, T.; Chen, S.; Jiang, S. Superlow Fouling Sulfobetaine and Carboxybetaine Polymers on Glass Slides. Langmuir 2006, 22, 10072-10077.
- (40) Wu, C.-J.; Huang, C.-J.; Jiang, S.; Sheng, Y.-J.; Tsao, H.-K. Superhydrophilicity and Spontaneous Spreading on Zwitterionic Surfaces: Carboxybetaine and Sulfobetaine. RSC Adv. 2016, 6 (30), 24827-24834.
- (41) Lowe, A. B.; McCormick, C. L. Synthesis and Solution Properties of Zwitterionic Polymers. Chem. Rev. 2002, 102 (11),
- (42) Schlenoff, J. B. Zwitteration: Coating Surfaces with Zwitterionic Functionality to Reduce Nonspecific Adsorption. Langmuir 2014, 30 (32), 9625-9636.
- (43) Birkner, M.; Ulbricht, M. Ultrafiltration Membranes with Markedly Different pH- and Ion-Responsivity by Photografted Zwitterionic Polysulfobetain or Polycarbobetain. J. Membr. Sci. 2015, 494, 57-67.
- (44) Yuan, J.; Zhang, J.; Zang, X.; Shen, J.; Lin, S. Improvement of Blood Compatibility on Cellulose Membrane Surface by Grafting Betaines. Colloids Surf., B 2003, 30 (1-2), 147-155.
- (45) Zheng, J.; He, Y.; Chen, S.; Li, L.; Bernards, M. T.; Jiang, S. Molecular Simulation Studies of the Structure of Phosphorylcholine Self-Assembled Monolayers. J. Chem. Phys. 2006, 125 (17), 174714.

- (46) Purdy, A. P.; Kuyinu, O. Synthesis and Dielectric Properties of Some Zwitterionic Polymers. *Polym. Prepr.* **2009**, *50* (2), *677*–*678*.
- (47) Hart, R.; Timmerman, D. New Polyampholytes: The Polysulfobetaines. J. Polym. Sci. 1958, 28 (118), 638–640.
- (48) Song, Y.; Doomes, E. E.; Prindle, J.; Tittsworth, R.; Hormes, J.; Kumar, C. S. S. R. Investigations into Sulfobetaine-Stabilized Cu Nanoparticle Formation: Toward Development of a Microfluidic Synthesis. *J. Phys. Chem. B* **2005**, *109* (19), 9330–9338.
- (49) Young, R. J.; Lovell, P. A. Introduction to Polymers, 3rd ed.; CRC Press: Boca Raton, FL, 2011.
- (50) Adamovsky, S. A.; Minakov, A. A.; Schick, C. Scanning Microcalorimetry at High Cooling Rate. *Thermochim. Acta* **2003**, 403 (1), 55–63.
- (51) Minakov, A. A.; Adamovsky, S. A.; Schick, C. Non-Adiabatic Thin-Film (Chip) Nanocalorimetry. *Thermochim. Acta* **2005**, 432 (2), 177–185.
- (52) Odian, G. Principles of Polymerization; Wiley: Hoboken, NJ, 2004; Vol. 4, p 832.
- (53) Asatekin, A.; Olivetti, E. a.; Mayes, A. M. Fouling Resistant, High Flux Nanofiltration Membranes from Polyacrylonitrile-graft-Poly(Ethylene Oxide). *J. Membr. Sci.* **2009**, 332 (1–2), 6–12.
- (54) Ratcharak, O.; Sane, A. Surface Coating with Poly-(Trifluoroethyl Methacrylate) Through Rapid Expansion of Supercritical CO2 Solutions. *J. Supercrit. Fluids* **2014**, *89*, 106–112.
- (55) Galin, M.; Marchal, E.; Mathis, A.; Meurer, B.; Soto, Y. M. M.; Galin, J. C. Poly(sulphopropylbetaines): 3. Bulk Properties. *Polymer* 1987, 28, 1937–1944.
- (56) Wu, T.; Beyer, F. L.; Brown, R. H.; Moore, R. B.; Long, T. E. Influence of Zwitterions on Thermomechanical Properties and Morphology of Acrylic Copolymers: Implications for Electroactive Applications. *Macromolecules* **2011**, *44* (20), 8056–8063.
- (57) Gauthier, S.; Duchesne, D.; Eisenberg, A. Vinylpyridinium Ionomers. 1. Influence of the Structure of the Ion on the State of Aggregation in Random Styrene-Based Systems. *Macromolecules* **1987**, 20, 753–759.
- (58) Duchesne, D.; Eisenberg, A. Vinylpyridinium Ionomers. III. Influence of the Matrix Glass Transition Temperature on the Dynamic Mechanical Properties of Random Acrylate-Based Systems. *Can. J. Chem.* 1990, *68*, 1228–1232.
- (59) Cebe, P.; Hu, X.; Kaplan, D. L.; Zhuravlev, E.; Wurm, A.; Arbeiter, D.; Schick, C. Beating the Heat Fast Scanning Melts Silk Beta Sheet Crystals. *Sci. Rep.* **2013**, *3*, 1130.
- (60) Cebe, P.; Partlow, B. P.; Kaplan, D. L.; Wurm, A.; Zhuravlev, E.; Schick, C. Using Flash DSC for Determining the Liquid State Heat Capacity of Silk Fibroin. *Thermochim. Acta* **2015**, *615*, 8–14.
- (1) Modestino, M. A.; Paul, D. K.; Dishari, S.; Petrina, S. A.; Allen, F. I.; Hickner, M. A.; Karan, K.; Segalman, R. A.; Weber, A. Z. Self-Assembly and Transport Limitations in Confined Nafion Films. *Macromolecules* 2013, 46 (3), 867–873.
- (62) Mauritz, K. A.; Moore, R. B. State of Understanding of Nafion. *Chem. Rev.* **2004**, *104*, 4535–4585.
- (63) Klein, D. Organic Chemistry, 2nd ed.; Wiley: Hoboken, NJ, 2013.
- (64) Inoue, Y.; Watanabe, J.; Ishihara, K. Dynamic Motion of Phosphorylcholine Groups at the Surface of Poly(2-Methacryloyloxyethyl Phosphorylcholine-random-2,2,2-Trifluoroethyl Methacrylate). *J. Colloid Interface Sci.* **2004**, 274 (2), 465–471.
- (65) Yang, R.; Jang, H.; Stocker, R.; Gleason, K. K. Synergistic Prevention of Biofouling in Seawater Desalination by Zwitterionic Surfaces and Low-Level Chlorination. *Adv. Mater.* **2014**, *26* (11), 1711–1718.
- (66) Yao, W.; Li, Y.; Huang, X. Fluorinated Poly(meth)acrylate: Synthesis and Properties. *Polymer* **2014**, *55* (24), 6197–6211.
- (67) Kobayashi, M.; Terayama, Y.; Yamaguchi, H.; Terada, M.; Murakami, D.; Ishihara, K.; Takahara, A. Wettability and Antifouling Behavior on the Surfaces of Superhydrophilic Polymer Brushes. *Langmuir* **2012**, 28 (18), 7212–7222.
- (68) Boussu, K.; Vandecasteele, C.; Van der Bruggen, B. Relation Between Membrane Characteristics and Performance in Nano-filtration. *J. Membr. Sci.* **2008**, 310 (1–2), 51–65.

- (69) Asatekin, A.; Mayes, A. M. Responsive Pore Size Properties of Composite NF Membranes Based on PVDF Graft Copolymers. *Sep. Sci. Technol.* **2009**, *44* (14), 3330–3345.
- (70) Asatekin, A.; Mayes, A. M. Oil Industry Wastewater Treatment with Fouling Resistant Membranes Containing Amphiphilic Comb Copolymers. *Environ. Sci. Technol.* **2009**, 43 (12), 4487–4492.